articles

molecular pharmaceutics

Targeted Proapoptotic Anticancer Drug Delivery System

Pooja Chandna,[†] Maha Saad,[†] Yang Wang,[†] Elizabeth Ber,[†] Jayant Khandare,[†] Alexandre A. Vetcher,[‡] Viatcheslav A. Soldatenkov,[§] and Tamara Minko*,[†]

Department of Pharmaceutics, Ernest Mario School of Pharmacy, Rutgers, The State University of New Jersey, Piscataway, New Jersey 08854, National Center for Biodefense and Infectious Diseases, George Mason University, Manassas, Virginia 20110, and Department of Radiation Medicine, Lombardi Comprehensive Cancer Center, Georgetown University Medical Center, Washington, D.C. 20007

Received May 3, 2007; Revised Manuscript Received June 28, 2007; Accepted July 5, 2007

Abstract: A novel targeted proapoptotic anticancer drug delivery system (DDS) was developed and evaluated both in vitro and in vivo. The system contains poly(ethylene glycol) polymer (PEG) as a carrier, camptothecin (CPT) as an anticancer drug/cell death inducer, a synthetic analogue of luteinizing hormone-releasing hormone (LHRH) peptide as a targeting moiety/penetration enhancer, and a synthetic analogue of BCL2 homology 3 domain (BH3) peptide as a suppressor of cellular antiapoptotic defense. The design of the multicomponent DDS allowed for a conjugation of one or two copies of each active ingredient (CPT, LHRH, and BH3) to one molecule of PEG carrier. The complex structure of the PEG conjugates was visualized at nanometer resolution using atomic force microscopy. We found that the ligand-targeted DDS for cancer cells preferentially accumulated in the tumor and allowed the delivery of active ingredients into the cellular cytoplasm and nuclei of cancer cells. Simultaneous apoptosis induction through the caspase-dependent signaling pathway and inhibition of cellular antiapoptotic defense by the suppression of BCL2 protein enhanced cytotoxicity and antitumor activity of the entire DDS to a level which could not be achieved by individual components applied separately. The DDS containing two copies of each active component (CPT, LHRH, and BH3) per molecule of PEG polymer had the highest anticancer efficiency in vitro and in vivo.

Keywords: Poly(ethylene glycol); camptothecin; LHRH; BH3; tumor targeting; antitumor activity; drug resistance; apoptosis

Introduction

Cancer is one of the leading causes of death in the United States. Although localized primary solid tumors can be successfully removed surgically, the treatment of spreading tumors and tumor metastases requires extensive chemotherapy. However, two main obstacles limit the success of chemotherapy: (1) severe adverse side effects on healthy organs and (2) development of drug resistance. The delivery of drugs as prodrugs specifically targeted to tumors and the suppression of cellular antiapoptotic defense can potentially be used to minimize the adverse side effects and suppress cellular resistance, respectively.

A prodrug is an inactive precursor of a drug which is converted into the active drug in the targeted organ, tissue, or cell.[1–7] Advantages of the prodrug approach include, but are not limited to, the prevention of systemic side effects, the increase in the bioavailability of the modified drug, and

* To whom correspondence should be addressed: Department of Pharmaceutics, Ernest Mario School of Pharmacy, Rutgers, The State University of New Jersey, 160 Frelinghuysen Rd., Piscataway, NJ 08854-8020. Phone: (732) 445-3831, ext. 214. Fax: (732) 445-3134. E-mail: minko@rci.rutgers.edu.

[†] Rutgers, The State University of New Jersey.

[‡] George Mason University.

[§] Georgetown University Medical Center.

(1) Duncan, R. The dawning era of polymer therapeutics. *Nat. Rev. Drug Discovery* **2003**, *2*, 347–360.

(2) Duncan, R.; Gac-Breton, S.; Keane, R.; Musila, R.; Sat, Y. N.; Satchi, R.; Searle, F. Polymer-drug conjugates, PDEPT and PELT: Basic principles for design and transfer from the laboratory to clinic. *J. Controlled Release* **2001**, *74*, 135–146.

10.1021/mp070053o CCC: $37.00
Published on Web 08/09/2007

the possibility of using specific organ, tissue, or cellular conditions to convert the inactive prodrug into its active form. In most cases, a prodrug includes a drug bound to (or encapsulated in) a water-soluble carrier. The more advanced type of prodrug [drug delivery system (DDS)] might include a targeting moiety and supplementary active ingredients in addition to the carrier and drug. The carrier combines all components of the DDS together and provides the required characteristics of the whole DDS, i.e., solubility, molecular mass, etc. A targeting moiety enforces the specific delivery of a drug to the targeted organ, tissue, or cell. Acting as a penetration enhancer, the targeting moiety also improves the cellular uptake of the entire DDS.

Active ingredients can be included in a complex DDS to augment the action of a main drug. These active ingredients may be drugs with different mechanisms of action or may provide an independent influence on cellular functions to promote effects of the drug. Frequently, separate components of the DDS are bound together by means of spacers. Such spacers play an important role by providing for the release of DDS components under certain conditions or at specific time points. In most cases, a spacer that binds a targeting moiety to the carrier is stable and nondegradable in body fluids and inside targeted cells. In contrast, spacers that connect a drug and other active components of the DDS to a carrier are usually biodegradable. The degradation of such spacers (or a bond between the spacer and a component) is normally caused by specific conditions inside the targeted organ, cell, or cellular organelles, providing additional "targeting" to specific intracellular compartments or organelles, such as the cytoplasm, mitochondria, nuclei, etc.[4,6,8–10] Recently, we proposed a novel type of branched citric acid spacer that allows for the simultaneous binding of several copies of different active ingredients to one polymeric carrier, therefore forming a prodrug with multivalent components.[6] This spacer minimizes steric hindrance of bound molecules and offers the choice of conjugation with compounds having -OH, -COOH, or -NH_2 functionality. In addition, each branch of a multivalent spacer can be connected to similar multivalent branched spacers, providing the possibility of increasing the number of active ingredients without a substantial increase in the molecular mass of the whole system.

Two types of targeting of an anticancer drug to tumors are generally used: (1) passive and (2) active targeting.[11] Passive targeting mainly utilizes the so-called enhanced permeability and retention (EPR) effect[12–14] responsible for the preferential accumulation of macromolecules in tumors. However, passive targeting by the EPR effect is only efficient for targeting of a high-molecular mass DDS to solid tumors and is not used for the selective delivery of anticancer drugs to spreading tumors, metastases, and types of cancer that do not form tumors. Several types of active targeting are currently being used to provide for the specific delivery of therapeutics to cancer cells.[11] The most effective and widely used approach is based on the coupling of a drug carrier with a targeting moiety specific to certain cancer cells. Many different types of targeting moieties are being used in experiments and clinical trials.[11,15–22] We proposed to employ a slightly modified synthetic analogue of luteinizing hormone-releasing hormone (LHRH) for the targeting of a DDS to cancer cells.[6,15,23,24] LHRH peptide provided for effective targeting of an active ligand to LHRH receptor-

(3) Greenwald, R. B.; Zhao, H.; Xia, J.; Wu, D.; Nervi, S.; Stinson, S. F.; Majerova, E.; Bramhall, C.; Zaharevitz, D. W. Poly(ethylene glycol) prodrugs of the CDK inhibitor, alsterpaullone (NSC 705701): Synthesis and pharmacokinetic studies. *Bioconjugate Chem.* **2004**, *15*, 1076–1083.

(4) Khandare, J.; Minko, T. Polymer-drug conjugates: Progress in polymeric prodrugs. *Prog. Polym. Sci.* **2006**, *31*, 359–397.

(5) Minko, T.; Khandare, J.; Jayant, S. Polymeric drugs. In *Macromolecular engineering: From precise macromolecular synthesis to macroscopic material properties and application*; Matyjaszewski, K., Gnanou, Y., Leibler, L., Eds.; Wiley-VCH Verlag GmbH & Co.: Weinheim, Germany, 2007; pp 2541–2595.

(6) Khandare, J. J.; Chandna, P.; Wang, Y.; Pozharov, V. P.; Minko, T. Novel polymeric prodrug with multivalent components for cancer therapy. *J. Pharmacol. Exp. Ther.* **2006**, *317*, 929–937.

(7) Khandare, J. J.; Jayant, S.; Singh, A.; Chandna, P.; Wang, Y.; Vorsa, N.; Minko, T. Dendrimer versus linear conjugate: Influence of polymeric architecture on the delivery and anticancer effect of paclitaxel. *Bioconjugate Chem.* **2006**, *17*, 1464–1472.

(8) Duncan, R. Designing polymer conjugates as lysosomotropic nanomedicines. *Biochem. Soc. Trans.* **2007**, *35*, 56–60.

(9) Duncan, R.; Cable, H. C.; Lloyd, J. B.; Rejmanova, P.; Kopecek, J. Degradation of side-chains of N-(2-hydroxypropyl)methacrylamide copolymers by lysosomal thiol-proteinases. *Biosci. Rep.* **1982**, *2*, 1041–1046.

(10) Minko, T. Drug targeting to the colon with lectins and neoglycoconjugates. *Adv. Drug Delivery Rev.* **2004**, *56*, 491–509.

(11) Minko, T.; Dharap, S. S.; Pakunlu, R. I.; Wang, Y. Molecular targeting of drug delivery systems to cancer. *Curr. Drug Targets* **2004**, *5*, 389–406.

(12) Maeda, H. The enhanced permeability and retention (EPR) effect in tumor vasculature: The key role of tumor-selective macromolecular drug targeting. *Adv. Enzyme Regul.* **2001**, *41*, 189–207.

(13) Fang, J.; Sawa, T.; Maeda, H. Factors and mechanism of "EPR" effect and the enhanced antitumor effects of macromolecular drugs including SMANCS. *Adv. Exp. Med. Biol.* **2003**, *519*, 29–49.

(14) Greish, K.; Fang, J.; Inutsuka, T.; Nagamitsu, A.; Maeda, H. Macromolecular therapeutics: Advantages and prospects with special emphasis on solid tumour targeting. *Clin. Pharmacokinet.* **2003**, *42*, 1089–1105.

(15) Dharap, S. S.; Qiu, B.; Williams, G. C.; Sinko, P.; Stein, S.; Minko, T. Molecular targeting of drug delivery systems to ovarian cancer by BH3 and LHRH peptides. *J. Controlled Release* **2003**, *91*, 61–73.

(16) Kopecek, J.; Kopeckova, P.; Minko, T.; Lu, Z. R.; Peterson, C. M. Water soluble polymers in tumor targeted delivery. *J. Controlled Release* **2001**, *74*, 147–158.

(17) Langer, M.; Beck-Sickinger, A. G. Peptides as carrier for tumor diagnosis and treatment. *Curr. Med. Chem.: Anti-Cancer Agents* **2001**, *1*, 71–93.

(18) Langer, R. Drug delivery. Drugs on target. *Science* **2001**, *293*, 58–59.

(19) Reubi, J. C. Peptide receptors as molecular targets for cancer diagnosis and therapy. *Endocr. Rev.* **2003**, *24*, 389–427.

(20) Torchilin, V. P. Drug targeting. *Eur. J. Pharm. Sci.* **2000**, *11* (Suppl. 2), S81–S91.

overexpressing cancer cells.[6,15,23,24] Simultaneously, it substantially limited the adverse drug side effects on healthy reproductive organs that have a lower level of expression of the receptors[15] and prevented drug accumulation in normal visceral organs, where LHRH receptors are not expressed detectably.[11,15,23–25] The LHRH receptor-targeted anticancer drug did not exhibit in vivo pituitary toxicity, did not significantly influence the time course or the plasma concentration of luteinizing hormone, and did not disturb the reproductive functions of mice.[24]

The most frequently used anticancer drugs have a dual effect on cancer cells. On one hand, they provoke cell death mainly by activation of the central apoptotic signal. On the other hand, they trigger antiapoptotic cellular defense primarily by inducing the overexpression of antiapoptotic members of the BCL2 protein family.[11,26] To prevent the activation of cellular defense and enhance the apoptosis induction, we proposed to include in the same DDS an anticancer drug with a synthetic analogue of BCL2 homology 3 (BH3) peptide or antisense oligonucleotides targeted to BCL2 mRNA.[11,15,25–27]

Our previous experimental data showed the effectiveness of LHRH peptide as an effective tumor targeting moiety and BH3 peptide as a suppressor of antiapoptotic cellular defense.[15,24,25] However, the separate use of only one peptide in the DDS was not able to eliminate both of the main obstacles of chemotherapy: adverse side effects and activation of cellular resistance. LHRH peptide enhanced the uptake of DDS by cancer cells and limited the accumulation of an anticancer drug in healthy tissues but did not prevent the overexpression of antiapoptotic members of the BCL2 protein family. BH3 peptide substantially enhanced the cytotoxicity of traditional chemotherapeutic drugs but was unable to prevent their accumulation in healthy organs, thus increasing the risk of adverse side effects. We hypothesize that only the simultaneous use of both LHRH and BH3 peptides in one drug delivery system will provide for concurrent tumor targeting and suppression of antiapoptotic cellular defense.[11,15] Such a multipronged attack on cancer will increase the efficacy of ovarian cancer therapy to an extent that cannot be achieved by individual components applied separately. This experimental work is aimed at verifying the hypothesis and designing, synthesizing, and evaluating in vitro and in vivo a novel multifunctional targeted proapoptotic drug delivery system which provides for the simultaneous tumor targeting by LHRH peptide, cell death induction by an anticancer drug camptothecin (CPT), and suppression of cellular antiapoptotic defense by BH3 peptide. The system also uses a novel multivalent branched spacer in combining several copies of active ingredients in one DDS to further enhance tumor targeting and cytotoxicity.

Experimental Section

Cell Line. The A2780 sensitive and A2780/AD multidrug resistant human ovarian carcinoma cell lines were obtained from T. C. Hamilton (Fox Chase Cancer Center, Philadelphia, PA). Cells were cultured in RPMI 1640 medium (Sigma, St. Louis, MO) supplemented with 10% fetal bovine serum (Fisher Chemicals, Fairlawn, NJ). Cells were grown at 37 °C in a humidified atmosphere of 5% CO_2 (v/v) in air. All experiments were performed on cells in the exponential growth phase.

Animal Tumor Model and Antitumor Activity. An animal model of human ovarian carcinoma xenografts was used as previously described.[24,25,28,29] Briefly, A2780 sensitive or A2780/AD multidrug resistant human ovarian cancer cells (2×10^6) were subcutaneously transplanted into the flanks of female athymic nu/nu mice. When the tumors reached a size of 0.3 cm^3 (15–20 days after transplantation), mice were treated intraperitoneally with saline (control); CPT; 1×CPT–PEG; 2×CPT–PEG; 1×CPT–PEG–1×LHRH; 1×CPT–PEG–1×BH3; 2×CPT–PEG–2×LHRH; 2×CPT–PEG–2×BH3; 1×CPT–PEG–1×BH3–1×LHRH; and 2×CPT–PEG–2×BH3–2×LHRH. Each experimental group consisted of 10 animals. The dose of all of the substances (10 mg/kg for the single injection) corresponded to the maximum tolerated dose of CPT. Equivalent CPT concentrations were 3 and 3.8 mg/kg for conjugates containing one and two copies of CPT, respectively. The maximum tolerated

(21) Yang, J.; Chen, H.; Vlahov, I. R.; Cheng, J. X.; Low, P. S. Characterization of the pH of Folate Receptor-Containing Endosomes and the Rate of Hydrolysis of Internalized Acid-Labile Folate-Drug Conjugates. *J. Pharmacol. Exp. Ther.* **2007**, *321*, 462–428.

(22) Henne, W. A.; Doorneweerd, D. D.; Hilgenbrink, A. R.; Kularatne, S. A.; Low, P. S. Synthesis and activity of a folate peptide camptothecin prodrug. *Bioorg. Med. Chem. Lett.* **2006**, *16*, 5350–5355.

(23) Dharap, S. S.; Minko, T. Targeted proapoptotic LHRH-BH3 peptide. *Pharm. Res.* **2003**, *20*, 889–896.

(24) Dharap, S. S.; Wang, Y.; Chandna, P.; Khandare, J. J.; Qiu, B.; Gunaseelan, S.; Sinko, P. J.; Stein, S.; Farmanfarmaian, A.; Minko, T. Tumor-specific targeting of an anticancer drug delivery system by LHRH peptide. *Proc. Natl. Acad. Sci. U.S.A.* **2005**, *102*, 12962–12967.

(25) Dharap, S. S.; Chandna, P.; Wang, Y.; Khandare, J. J.; Qiu, B.; Stein, S.; Minko, T. Molecular targeting of BCL2 and BCLXL proteins by synthetic BH3 peptide enhances the efficacy of chemotherapy. *J. Pharmacol. Exp. Ther.* **2006**, *316*, 992–998.

(26) Minko, T.; Dharap, S. S.; Fabbricatore, A. T. Enhancing the efficacy of chemotherapeutic drugs by the suppression of antiapoptotic cellular defense. *Cancer Detect. Prev.* **2003**, *27*, 193–202.

(27) Pakunlu, R. I.; Wang, Y.; Tsao, W.; Pozharov, V.; Cook, T. J.; Minko, T. Enhancement of the efficacy of chemotherapy for lung cancer by simultaneous suppression of multidrug resistance and antiapoptotic cellular defense: Novel multicomponent delivery system. *Cancer Res.* **2004**, *64*, 6214–6224.

(28) Minko, T.; Kopeckova, P.; Kopecek, J. Efficacy of the chemotherapeutic action of HPMA copolymer-bound doxorubicin in a solid tumor model of ovarian carcinoma. *Int. J. Cancer* **2000**, *86*, 108–117.

(29) Pakunlu, R. I.; Wang, Y.; Saad, M.; Khandare, J. J.; Starovoytov, V.; Minko, T. In vitro and in vivo intracellular liposomal delivery of antisense oligonucleotides and anticancer drug. *J. Controlled Release* **2006**, *114*, 153–162.

dose of CPT was estimated in separate experiments on the basis of the animal weight change after the injection of increasing doses of CPT as previously described.[24,25,28,29] Tumor size was measured 24, 48, 72, and 96 h after the treatment. Animal weight was measured every day. Changes in tumor size were used as an overall marker for antitumor activity as previously described.[24,25,28,29]

Synthesis of Conjugates. CPT, *N*,*N*-diisopropylethylamine, and 4-(methylamino)pyridine (DMAP) were obtained from Sigma Chemical Co. (Atlanta, GA); bis(2-carboxyethyl)PEG polymer and fluorescein isothiocyanate (FITC) were obtained from Fluka (Allentown, PA). LHRH analogue, Lys6-des-Gly10-Pro9-ethylamide (Gln-His-Trp-Ser-Tyr-D-Lys-Leu-Arg-Pro-NH-Et), and BH3 (Ac-Met-Gly-Gln-Val-Gly-Arg-Gln-Leu-Ala-Ile-Ile-Asn-Arg-Arg-Tyr-Cys-NH_2) peptides were synthesized according to our design by American Peptide Co. (Sunnyvale, CA).[15] The α,ω-bis(2-carboxyethyl)PEG–citric acid conjugate was synthesized as previously described.[6] Near-infrared fluorophore cyanine dye Cy5.5 was obtained from Amersham Biosciences (Piscataway, NJ).

α,ω-Bis(2-carboxyethyl)PEG–Citric Acid–CPT Conjugates. Conjugates were prepared by dissolving the α,ω-bis(2-carboxyethyl)PEG–citric acid conjugate (molecular mass of∼3382.24 Da, 50 mg, 0.0147 mM) and CPT (5.2 mg, 0.0147 mM) in 5 mL of anhydrous DMSO and 10 mL of anhydrous DCM. The reaction mixture was allowed to stir at room temperature for 30 min. EDC·HCl (3 mg, 0.0156 mM) was added to the reaction mixture which served as condensing agent, and the catalyst DMAP (2.0 mg, 0.016 mM) was also added. The reaction mixture was continuously stirred at room temperature for 48 h. The carbodiimide urea formed during the reaction was removed by filtration. The unreacted EDC·HCl and CPT were also removed using Spectra/Por dialysis membrane (molecular mass cutoff, ∼2000 Da) using DMSO as a solvent. The conjugate was dried under a vacuum at room temperature. Likewise, the conjugates with two copies of CPT were prepared by using two molar ratios of CPT and EDC·HCl.

α,ω-Bis(2-carboxyethyl)PEG–Citric Acid–CPT–LHRH Conjugates. The α,ω-bis(2-carboxyethyl)PEG3000–CA–1CPT conjugate (molecular mass of ∼3729 Da, 50 mg, 0.0134 mM) and peptide LHRH-NH_2 (18 mg, 0.013 mM) were dissolved in 3 mL of anhydrous DMSO and 12 mL of anhydrous DCM. The reaction mixture was allowed to stir for 30 min. EDC·HCl (3.0 mg, 0.0134 mM) was added to the solution described above as a condensing agent, and the catalyst DMAP (1.0 mg, 0.008 mM) was also added. The further steps were similar to the synthesis of the PEG–citric acid–CPT conjugate described above. In addition, the polymer conjugates with two copies of the LHRH-NH_2 peptide were prepared using two molar ratios of LHRH-NH_2 and EDC·HCl.

α,ω-Bis(2-carboxyethyl)PEG–Citrate–CPT–LHRH–BH3 Conjugates. The α,ω-bis(2-carboxyethyl)PEG–citrate–CPT–LHRH conjugate (molecular mass of ∼6421 Da, 294 mg, 0.04578 mM) and BH3 peptide (106.20 mg, 0.04578 mM) were dissolved in 4 mL of DMSO and 10 mL of DCM. The reaction mixture was stirred for 30–40 min. EDC·HCl (8.74 mg, 0.045778 mM) was added to the reaction mixture described above as a condensing agent, and the catalyst DMAP (1.0 mg, 0.08 mM) was also added. The further steps were similar to those of the synthesis of the PEG–citric acid–CPT conjugate described above. The conjugate with two copies of the BH3 peptide was prepared by using two molar ratios of BH3 and EDC·HCl.

Synthesis of Cy5.5–PEG Conjugates. Bis-diamine PEG was purchased from NOF Corp. with a molecular mass of 3677 Da. Near-infrared fluorophore cyanine dye Cy5.5 NHS ester (1.0 mg) was dissolved in 1.0 mL of DMF and bis-PEG amine (9.0 mg) was separately dissolved in 1.0 mL of DMF. Triethanolamine (0.5 mL) was added to the Cy5.5 solution to activate the Cy5.5 NHS ester. Furthermore, the PEG solution was added to Cy5.5 ester and stirred continuously for 4 h at room temperature. The reaction mixture was protected from the light. Free Cy5.5 was removed with a SpectraPore dialysis membrane with a cutoff of 2000 Da. In addition, further purification was carried out with a Sephadex G10 column. Conjugate was dried under vacuum at room temperature.

Synthesis of the Cy5.5–PEG–LHRH Conjugate. The conjugate prepared as mentioned above resulted with one free amine at the terminus and was coupled with succinic acid (SA) to yield Cy5.5–PEG–COOH (CP). Briefly, CP and SA were dissolved in 3.0 mL of anhydrous DMSO and 5.0 mL of anhydrous DCM. The molar ratio of CP to SA was maintained at 1:1. EDC·HCl was added as a coupling agent, and DMAP was used as a catalyst; 0.4 mL of triethylamine base was added to remove the salt from the coupling agent. The reaction mixture was stirred continuously for 24 h at room temperature. The resulting solution was filtered to remove DCU, and the filtrate was dialyzed extensively with anhydrous DMSO (dialysis membrane with a molecular mass cutoff of 2000 Da) for 24 h to remove unreacted SA and EDC·HCl. Furthermore, the conjugate was purified using a size exclusion Sephadex G10 column. Conjugate was dried under the vacuum at room temperature. Additionally, LHRH-NH_2 was conjugated with the resulting CP–SA conjugate to form an amide conjugate. LHRH-NH_2 and CP–SA conjugate were dissolved in 4.0 mL of anhydrous DMSO and 6.0 mL of anhydrous DCM. The molar ratio of LHRH NH_2 to CP-SA was maintained at 1:1. EDC·HCl was added as a coupling agent, and DMAP was used as a catalyst; 0.4 mL of triethylamine base was added to remove the salt from the coupling agent. The reaction mixture was stirred continuously for 24 h at room temperature. The resulting solution was filtered to remove DCU, and the filtrate was dialyzed extensively with anhydrous DMSO (dialysis membrane with a molecular mass cutoff of 2000 Da) for 24 h to remove unreacted SA and EDC·HCl. The conjugate was purified using a size exclusion Sephadex G10 column and dried under vacuum at room temperature.

Cellular Internalization of Polymers. To analyze cellular internalization of different molecular mass polymers, PEG polymers were labeled with fluorescein isothiocyanate (FITC)

as previously described.[7] Cellular internalization of FITC-labeled PEG polymers in living cells was studied by confocal microscopy at 37 °C within 4.5 h.

Atomic Force Microscopy. Atomic force microscopy (AFM) imaging of PEG conjugates was conducted in tapping mode which is generally described elsewhere.[30] Briefly, 50 μL of the PEG conjugate suspension in water was applied on freshly cleaved mica which was kept for 10 min at 100% humidity to achieve particle deposition. After we removed the excess water by gently touching the side of mica with a piece of filter paper, we dried PEG conjugates under nitrogen. The images were acquired in air with a Nanoscope III AFM instrument (Veeco/Digital Instruments, Santa Barbara, CA) using tapping mode-etched OMCL-AC160TS silicon probes (Olympus Optical Co., Tokyo, Japan).[31] The images were processed, and the measurements were performed with Femtoscan version 2.2.85(5.1) (Advanced Technologies Center, Moscow, Russia). For statistical purposes, no fewer than 50 unobstructed PEG polymer conjugates were analyzed.

In Vivo Imaging. To assess the distribution of PEG polymers in the body, polymers were labeled with Cy5.5 as described above. In vivo distribution of Cy5.5-labeled targeted and nontargeted conjugates was studied using the IVIS Imaging System (Xenogen, Alameda, CA) in anesthetized animals according to the manufacturer's instructions. Animals were anesthetized with isoflurane using the XGI-8 Gas Anesthesia System (Xenogen). Visible light and fluorescent images were taken and overlaid using the manufacturer's software to obtain a composite image.

Organ Distribution. Aliquots of PEG and LHRH–PEG conjugates were radiolabeled with tritium. Radiolabeling was done on LHRH–PEG-NH_2 or PEG-NH_2 with [^{3}H]acetic anhydride in the presence of 1% diisopropylethyl amine and methanol to yield LHRH–PEG-NH-CO-CH_3-[^{3}H] and PEG–NH-CO-CH_3-[^{3}H] conjugates, respectively. The distribution in tumor and organ (liver, kidney, spleen, heart, lung, brain, and pituitary) of radiolabeled conjugates was studied in nude nu/nu mice. Twelve mice were used in this experiment. Six mice were used as a control, while xenografts of human ovarian cancer were transplanted in the rest. When the tumors reached a size of 1 cm^3 (15–20 days after inoculation), mice were treated intraperitoneally with 10 mg of the desired conjugate/kg. The maximum tolerated dose was detected in separate experiments. Mice without a tumor have received the same dose of conjugates.

Cytotoxicity. The cytotoxicity of all studied conjugates and free CPT was assessed using a modified MTT [3-(4,5-dimethylthiazol-2-yl)-2,5-diphenyltetrazolium bromide] assay as previously described.[27,32]

Protein Expression. The identification of BCL2 and caspase 9 proteins was done by Western immunoblotting analysis and processed using scanning densitometry to quantify the expressed protein. To this end, harvested cells were lysed in Ripa buffer (Santa Cruz Biotechnologies, Inc., Santa Cruz, CA) using a small gauge needle (27 gauge) and syringe. Following incubation on ice for 45 min, the cells were centrifuged at 10000*g* for 10 min. The protein content in the supernatant was determined using the BCA protein assay kit (Pierce, Rockford, IL), and 50 μg of protein was run on a 15% sodium dodecyl sulfate (SDS)–polyacrylamide gel immersed in Tris/glycine/SDS buffer (Bio-Rad, Hercules, CA) for 90 min at 70 V. Proteins were transferred to an Immobilon-P nitrocellulose membrane (Millipore, Bedford, MA) in a Tris/glycine buffer (Bio-Rad) for 90 min at 100 V. The membrane was blocked in nonfat milk for 30 min at room temperature on a rotating shaker to prevent nonspecific binding, washed, and incubated overnight with anti-BCL2 rabbit primary antibody (1:250 dilution, Stress Gene Biotechnologies, Victoria, BC), anti-caspase 9 rabbit primary antibody (1:500 dilution, Stress Gen Biotechnologies, Victoria, BC), or anti-β-actin mice primary antibody (1:2000 dilution, Oncogene Research, San Diego, CA) at 4 °C. After being washed further, the membrane was immersed in goat anti-rabbit and goat anti-mouse IgG biotinylated antibody (1:3000 and 1:1000 dilution, respectively; Bio-Rad) at room temperature for 1.5 h on a rotating shaker. Bands were visualized using an alkaline phosphatase color development reagent (Bio-Rad). The bands were digitally photographed and scanned using the Gel Documentation System 920 (NucleoTech, San Mateo, CA). β-Actin was used as an internal standard to normalize protein expression. Band intensities of BCL2 protein and caspase 9 are expressed as the percentage of the β-actin band intensity, which was set at 100%.

Apoptosis. The induction of apoptosis was analyzed by the measurement of the enrichment of histone-associated DNA fragments (mono- and oligonucleosomes) in homogenates of the tumor using antihistone and anti-DNA antibodies by a cell death detection ELISA Plus kit (Roche, Nutley, NJ) as previously described.[24,25,27,29]

Statistical Analysis. Data that were obtained were analyzed using descriptive statistics and single-factor analysis of variance (ANOVA) and presented as mean values ± the standard deviation (SD) from four to eight independent measurements in separate experiments.

Results

Cellular Internalization of Polymers. To study cellular internalization of polymers, poly(ethylene glycol) with

(30) Leclere, P.; Hennebicq, E.; Calderone, A.; Brocorens, P.; Grimsdale, A.; Mullen, K.; Bredas, J.; Lazzaroni, R. Supramolecular organization in block copolymers containing a conjugated segment: A joint AFM/molecular modeling study. *Prog. Polym. Sci.* **2003**, *28*, 55–81.

(31) Vetcher, A.; Srinivasan, S.; Vetcher, I.; Abramov, S.; Kozlov, M.; Baughman, R.; Levene, S. Fractionation of SWNT/nucleic acid complexes by agarose gel electrophoresis. *Nanotechnology* **2006**, *17*, 4263–4269.

(32) Minko, T.; Kopeckova, P.; Pozharov, V.; Kopecek, J. HPMA copolymer bound adriamycin overcomes MDR1 gene encoded resistance in a human ovarian carcinoma cell line. *J. Control. Release* **1998**, *54*, 223–233.

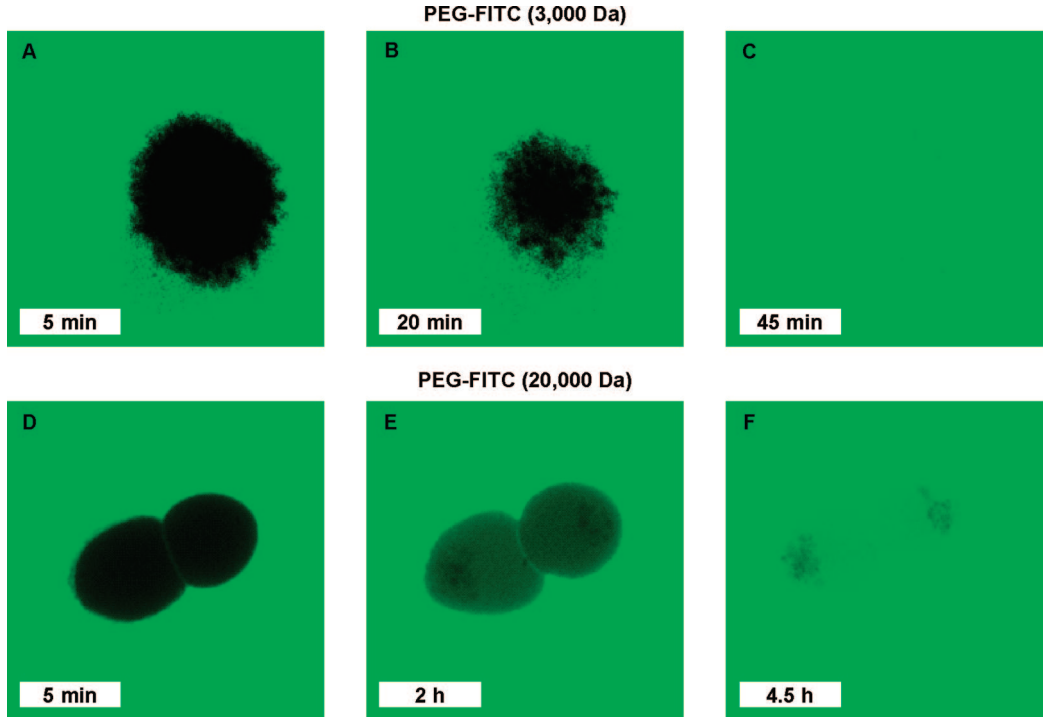

Figure 1. Intracellular internalization of different molecular mass PEG polymers [(A–C) low- and (D–F) high-molecular mass polymers]. Images of FITC-labeled polymers were taken by a confocal microscope in living cells at 37 °C within different time points after the exposure.

different molecular masses was labeled with FITC. Labeled polymers were visualized in living cells with a confocal microscope at 37 °C within different time intervals. Two labeled PEG polymers with molecular masses of 3000 and 20 000 Da were used. Intensive internalization of lower-molecular mass polymer started 20 min after the beginning of incubation (Figure 1B). Forty-five minutes after the beginning of the exposure, 3000 Da FITC-labeled polymer was distributed almost homogeneously within the cancer cell (Figure 1C). Intensive fluorescence, comparable with fluorescence in the medium, was seen both in the cellular cytoplasm and in nuclei. These data show that PEG polymer with molecular mass of 3000 Da easily penetrates cellular cytoplasm and nuclei. In contrast, the internalization of PEG polymer with a molecular mass of approximately 20 000 Da occurred much slower when compared with that of the smaller polymer (3000 Da). A considerable accumulation of polymer in the cellular cytoplasm occurred 2–4.5 h after the addition of the polymer to the medium (Figure 1E,F).

Atomic Force Microscope Imaging of DDS. To assess the shape, size, and morphology of PEG conjugates, we employed AFM, a technology that allows direct visualization of biopolymers, such as DNA and proteins, and various drug delivery polymer particles at nanometer resolution.[31,33] AFM imaging revealed the complex structure of conjugates visible as compact (30–50 nm) particles with distal protrusions

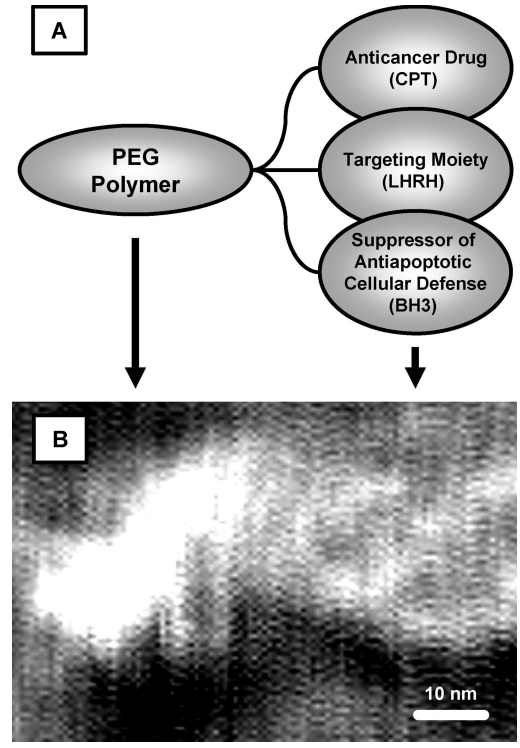

Figure 2. Schematic structure (A) and representative atomic force microscope image (B) of PEG conjugates on a mica surface in tapping mode.

(Figure 2). Although detailed organization of conjugates at the molecular level has to be further investigated, AFM images provide initial evidence of nanosized dimensions and a predicted complex molecular structure of PEG conjugates.

(33) Lonskaya, I.; Potaman, V. N.; Shlyakhtenko, L. S.; Oussatcheva, E. A.; Lyubchenko, Y. L.; Soldatenkov, V. A. Regulation of poly(ADP-ribose) polymerase-1 by DNA structure-specific binding. *J. Biol. Chem.* **2005**, *280*, 17076–17083.

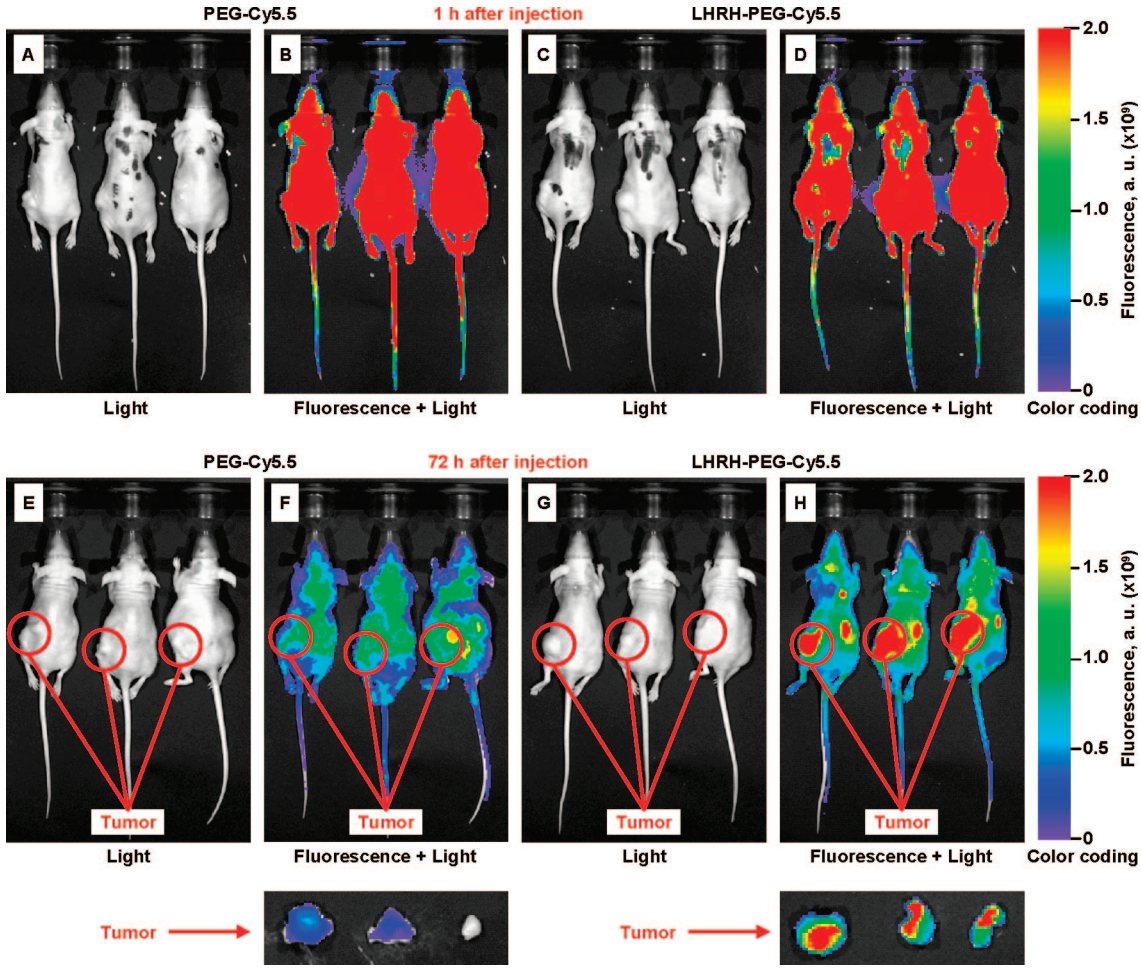

Figure 3. Typical in vivo images of mice bearing xenografts of A2780 human ovarian carcinoma. Mice were injected with PEG (A, B, E, and F) and PEG–LHRH (C, D, G, and H) polymers labeled with near-infrared fluorophore cyanine dye (Cy5.5). Images were taken using the IVIS Imaging System (Xenogen) in anesthetized animals 1 and 72 h after injection of polymer. Tumors were excised 72 h after the treatment and imaged. Visible light (A, C, E, and G) and fluorescent images were overlaid to obtain composite images (B, D, F, and H).

Body Distribution of Targeted and Nontargeted Polymers. To investigate the distribution of PEG polymers in mice, we labeled the polymers with near-infrared dye Cy5.5. Conjugates were visualized in anesthetized live animals using an IVIS imaging system. The system uses color coding of fluorescence with blue coding for low levels of fluorescence and red color for high levels. The results (Figure 3) show that both targeted and nontargeted polymers provide for a relatively long circulation in the bloodstream. Actually, a fairly high blood level of both conjugates was registered 72 h after the injection, resulting in a comparable level of fluorescence (green-blue color of the composite image in Figure 3F,H). However, body distribution and tumor accumulation of targeted and nontargeted conjugates substantially differed. Targeted conjugate predominantly accumulated in the tumor (Figure 3H), while the distribution of nontargeted PEG was more homogeneous (Figure 3F). Qualitative imaging data are supported by a quantitative measurement of the PEG distribution using a radioactive conjugate labeling of the polymer (Figure 4). The analysis of organ distribution of the radioactively labeled nontargeted (Figure 4A) and tumor-targeted conjugates (Figure 4B) shows preferential accumulation of LHRH-targeted conjugate in the tumor (Figure 4B). It should be stressed that significant fractions of targeted conjugate accumulated in healthy ovaries of animals bearing subcutaneous xenografts of human ovarian tumor.

In Vitro Cytotoxicity. Cytotoxicity data (Figure 5) showed that the conjugation to the PEG polymer, inclusion in the anticancer drug delivery system of a targeting moiety (LHRH peptide), and a suppressor of antiapoptotic cellular resistance (BH3 peptide) to the drug delivery system significantly increased the cytotoxicity of CPT. Moreover, an increase in the number of copies of the drug and peptides per molecule of the polymer led to further enhancement of the anticancer efficacy of camptothecin.

Suppression of Antiapoptotic Cellular Defense and Enhancement of Apoptosis Induction. As expected, an incorporation of BH3 peptide into the CPT-containing DDS

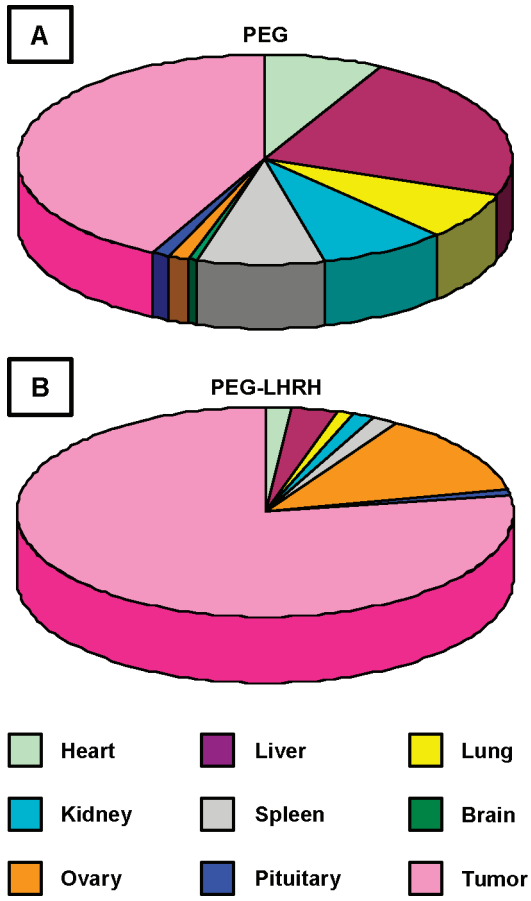

Figure 4. Distribution of tritium-labeled PEG (A) and PEG–LHRH conjugate (B) in different tissues of mice bearing xenografts of A2780 human ovarian carcinoma. Radioactivity in each tissue is expressed as a percentage of the total.

prevented the overexpression of BCL2 protein by an anticancer drug and even suppressed the level of this protein in ovarian tumor cells (Figure 6A). The suppression led to the inhibition of antiapoptotic cellular defense and, therefore, to the enhancement of the activation of caspase 9, the main initiator of apoptosis (Figure 6B,C). In turn, caspase activation initiated a proapoptotic signal and apoptosis itself (Figure 7). It should be stressed that the proposed DDS induced apoptosis in both drug sensitive (Figure 7A) and multidrug resistant (Figure 7B) ovarian tumors. However, apoptosis in resistant tumors was less pronounced (compare panels A and B of Figure 7).

Antitumor Activity. The measurement of tumor size in mice bearing xenografts of sensitive and multidrug resistant human ovarian carcinomas showed that simultaneous tumor targeting by the LHRH peptide, cell death induction by CPT, and suppression of antiapoptotic cellular defense by BH3 peptide led to the high antitumor activity of the entire DDS (Figure 8). The system containing two copies each of CPT, LHRH, and BH3 was the most effective in the suppression of tumor growth in both sensitive (Figure 8A, bar 10) and multidrug resistant tumors (Figure 8B, bar 10).

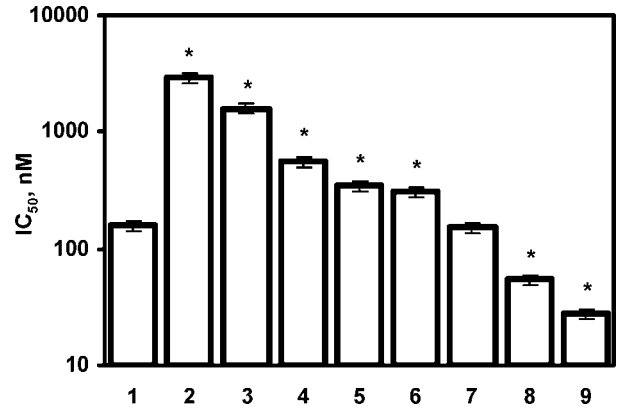

Figure 5. Cytotoxicity of CPT (1), 1×CPT–PEG (2), 2×CPT–PEG (3), 1×CPT–PEG–1×LHRH (4), 1×CPT–PEG–1×BH3 (5), 2×CPT–PEG–2×LHRH (6), 2×CPT–PEG–2×BH3 (7), 1×CPT–PEG–1×BH3–1×LHRH (8), and 2×CPT–PEG–2×BH3–2×LHRH (9) in A2780 human ovarian carcinoma cells. Cells were incubated for 48 h with 45 different equivalent CPT concentrations. Means ± SD are shown. An asterisk indicates that $P < 0.05$ when compared with the CPT value.

Discussion

The main goal of this experimental work was to develop, synthesize, and evaluate in vitro and in vivo a novel, highly effective anticancer drug delivery system. It was expected that this system would satisfy the following requirements. First, it should provide targeted delivery of active ingredients specifically to the tumor cells, preventing drug accumulation in healthy organs and therefore limiting adverse side effects of the treatment. Second, this DDS should effectively induce cell death in cancer cells. Third, the system should prevent the development of cellular drug resistance after the treatment with an anticancer drug. Fourth, the architecture of the DDS should allow for the easy addition of several copies of active ingredients per molecule of the carrier. To fulfill these demands, the targeted proapoptotic anticancer delivery system was designed, synthesized, and evaluated. The system contains a carrier (PEG polymer) and one or two copies of each active component: an anticancer drug (CPT), a targeting moiety (LHRH peptide), and a suppressor of antiapoptotic cellular defense (BH3 peptide). The carrier combines all components together providing for a high solubility of the entire DDS. The targeting moiety allows for tumor targeting and a specific uptake of the DDS by cancer cells through the interaction of targeting peptide with corresponding receptors overexpressed in cancer cells. The anticancer drug induces cell death (CPT), and the suppressor of antiapoptotic cellular defense (BH3) prevents the development of drug resistance in cancer cells.

We selected a polymer with a molecular mass of 3000 Da on the basis of the following considerations. First, even without a cell targeting moiety (LHRH), low-molecular mass PEG can easily penetrate through the cellular plasma membrane and be distributed homogeneously inside cancer

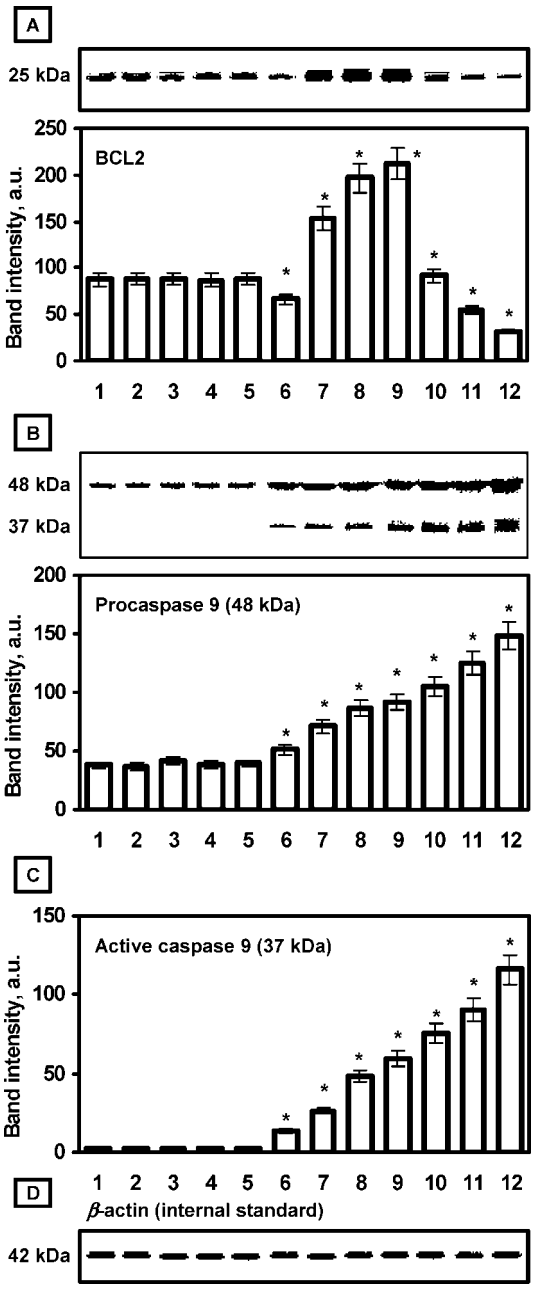

Figure 6. Typical images of Western blots of BCL2 (A), caspase 9 (B and C), and β-actin (D, internal standard) proteins and densitometric analysis of bands in tumor tissues isolated from mice bearing xenografts of A2780 human ovarian carcinoma. Mice were treated with the indicated formulations. Band intensities of BCL2 and caspase 9 proteins are expressed as the percentage of the β-actin band intensity, which was set to 100%. Means $\pm$ SD are shown. An asterisk indicates $P < 0.05$ when compared with control: (1) control (saline), (2) LHRH, (3) BH3, (4) PEG, (5) PEG–1×LHRH, (6) PEG–1×BH3, (7) CPT, (8) 1×CPT–PEG, (9) 1×CPT–PEG–1×LHRH, (10) 1×CPT–PEG–1×BH3, (11) 1×CPT–PEG–1×BH3–1×LHRH, (12) 2×CPT–PEG–2×BH3–2×LHRH.

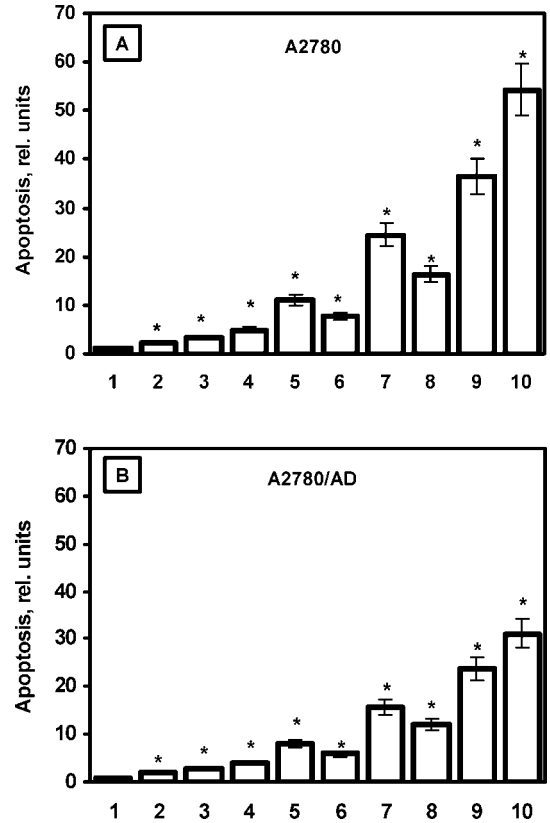

Figure 7. Apoptosis induction in tumor tissues isolated from mice bearing xenografts of sensitive A2780 (A) and multidrug resistant A2780/AD (B) human ovarian carcinoma cells. Mice were treated with indicated formulations. The enrichment of histone-associated DNA fragments (mono- and oligonucleotides) in control mice was set to unit 1, and the degree of apoptosis was expressed in relative units. Mice were treated with the indicated formulations. Means $\pm$ SD are shown. An asterisk indicates $P < 0.05$ when compared with control: (1) control (saline), (2) CPT, (3) 1×CPT–PEG, (4) 2×CPT–PEG, (5) 1×CPT–PEG–1×LHRH, (6) 1×CPT–PEG–1×BH3, (7) 2×CPT–PEG–2×LHRH, (8) 2×CPT–PEG–2×BH3, (9) 1×CPT–PEG–1×BH3–1×LHRH, and (10) 2×CPT–PEG–2×BH3–2×LHRH.

cells. Although the strong penetration ability of PEG polymers of a relatively small molecular mass sounds obvious, its easy penetration through the plasma membrane and homogenous distribution through the cancer cell, including the cellular nucleus, were first documented experimentally in this study. It is possible that PEG polymer penetrates the plasma membrane of cancer cells by endocytosis like other water-soluble polymers.[34] Second, polymers with higher molecular masses exhibit pronounced passive targeting through the EPR effect.[12–14,35] Therefore, to ensure that specific tumor accumulation of targeted LHRH–PEG conjugates is due to the inclusion of LHRH peptide as a tumor

(34) Jensen, K. D.; Nori, A.; Tijerina, M.; Kopeckova, P.; Kopecek, J. Cytoplasmic delivery and nuclear targeting of synthetic macromolecules. *J. Control. Release.* **2003**, *87*, 89–105.

(35) Matsumura, Y.; Maeda, H. A new concept for macromolecular therapeutics in cancer chemotherapy: mechanism of tumoritropic accumulation of proteins and the antitumor agent smancs. *Cancer Res.* **1986**, *46*, 6387–6392.

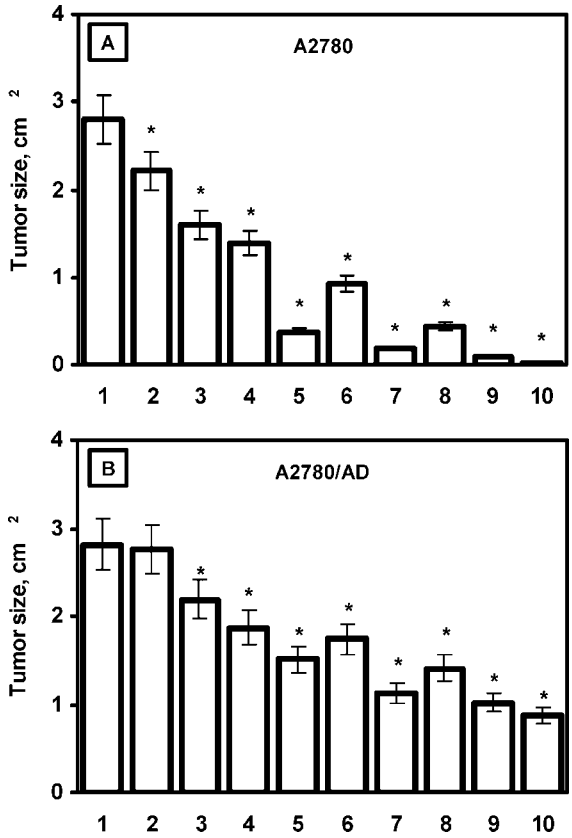

Figure 8. Tumor size in mice bearing xenografts of sensitive A2780 (A) and multidrug resistant A2780/AD (B) human ovarian carcinoma cells. Mice were treated with the indicated formulations. Tumor size was measured 96 h after the treatment. Means ± SD are shown. An asterisk indicates $P < 0.05$ when compared with control: (1) control (saline), (2) CPT, (3) 1×CPT–PEG, (4) 2×CPT–PEG, (5) 1×CPT–PEG–1×LHRH, (6) 1×CPT–PEG–1×BH3, (7) 2×CPT–PEG–2×LHRH, (8) 2×CPT–PEG–2×BH3, (9) 1×CPT–PEG–1×BH3–1×LHRH, and (10) 2×CPT–PEG–2×BH3–2×LHRH.

targeting moiety and not the result of the EPR effect, we used a relatively small PEG polymer (3000 Da) as a carrier. The visualization of the DDS with an atomic force microscope revealed a compact structure of PEG polymer with a size of 30–50 nm conjugated with a distant tree-armed citric acid multifunctional spacer containing globules of active ingredients (LHRH, CPT, and BH3). The imaging verifies the predicted structure of synthesized polymers.

The data obtained in this study about the distribution of targeted and nontargeted polymers support previously reported data about the body distribution of similar polymers obtained in our experiments by a different method.[24] It is interesting that the average blood concentrations (proportional to the registered fluorescence of labeled conjugates) were comparable for both targeted and nontargeted conjugates 1 and 72 h after the injection, resulting in similar distribution and/or coloring of the images. At the same time, the level of tumor accumulation of the targeted conjugate was substantially higher in the tumor when compared with the level of accumulation of the nontargeted conjugate. This finding allows us to speculate that a considerable part of the injected dose of nontargeted conjugate was expelled from the organism within 72 h, while the targeted conjugate remained in the tumor and therefore was not eliminated from the body of the experimental animals. Such retention forms a prerequisite for higher antitumor activity and weakens the adverse side effects of the targeted conjugate. The qualitative imaging data were supported by the quantitative measurement of conjugate accumulation using radioactive labeling of the conjugates. Experimental data showed that a significant part of the injected dose of targeted polymer accumulated in ovaries of experimental animals where the LHRH receptors were also expressed, although at a level lower than that in ovarian tumor.[15] This accumulation should not raise concerns about adverse effects of the LHRH-targeted conjugate on the female reproductive system. First, such adverse effects might not be taken into consideration because ovaries are usually surgically removed in females with ovarian and sometimes breast cancer (the main types of cancer that are prospective candidates for LHRH-targeted chemotherapy in females).[36–39] Moreover, our previous data showed that similar treatment did not lead to the disturbances in the time course of luteinizing hormone and reproductive functions in female mice[24] We also previously showed that LHRH-targeted PEG conjugates did not impose pituitary toxicity probably because of the protection of the pituitary gland by the blood–brain barrier which is impermeable for the conjugate that was used.[24]

We found that a DDS that simultaneously combines a targeting moiety, an inhibitor of antiapoptotic cellular defense, and an anticancer drug exhibits cytotoxicity much higher than that of free drug. Such enhancement in the toxicity reflects several mechanisms. First, conjugation of CPT to highly water-soluble PEG polymer substantially increases its aqueous solubility. Second, the interaction of the LHRH peptide with corresponding receptors initiates receptor-mediated endocytosis and therefore enhances the uptake of the entire DDS by cancer cells. Third, the suppression of antiapoptotic cellular defense by the BH3 peptide weakens the cell death induction ability of the

(36) Rocca, W. A.; Grossardt, B. R.; de Andrade, M.; Malkasian, G. D.; Melton, L. J. 3rd Survival patterns after oophorectomy in premenopausal women: a population-based cohort study. *Lancet Oncol* **2006**, *7*, 821–8.

(37) Jakesz, R. An update on ovarian suppression/ablation. *Int J Gynecol Cancer* **2006**, *16* (Suppl 2), 511–4.

(38) Schmeler, K. M.; Sun, C. C.; Bodurka, D. C.; White, K. G.; Soliman, P. T.; Uyei, A. R.; Erlichman, J. L.; Arun, B. K.; Daniels, M. S.; Rimes, S. A.; Peterson, S. K.; Slomovitz, B. M.; Milam, M. R.; Gershenson, D. M.; Lu, K. H. Prophylactic bilateral salpingo-oophorectomy compared with surveillance in women with BRCA mutations. *Obstet Gynecol* **2006**, *108*, 515–20.

(39) Domchek, S. M.; Friebel, T. M.; Neuhausen, S. L.; Wagner, T.; Evans, G.; Isaacs, C.; Garber, J. E.; Daly, M. B.; Eeles, R.; Matloff, E.; Tomlinson, G. E.; Van't Veer, L.; Lynch, H. T.; Olopade, O. I.; Weber, B. L.; Rebbeck, T. R. Mortality after bilateral salpingo-oophorectomy in BRCA1 and BRCA2 mutation carriers: a prospective cohort study. *Lancet Oncol* **2006**, *7*, 223–9.

anticancer drug. The toxicity of the conjugates rose with the increase in the number of copies of LHRH and BH3 peptides conjugated with one molecule of PEG polymer. The number of copies of BH3 peptide and CPT is limited by the low solubility of the drug and the peptide. It is possible to attach more than two copies of LHRH peptide to one molecule of PEG polymer. However, our preliminary data showed that further increases in the number of LHRH copies does not result in the additional increase of tumor targeting. This most likely reflects the fact that the number of LHRH receptors per cancer cell is limited and almost all vacancies can be filled out by the conjugate containing two or three copies of LHRH peptide per molecule of carrier. Therefore, the 2× CPT–PEG, 2× BH3, 2× LHRH configuration of the drug delivery system most likely represents an optimal configuration of a DDS providing for the highest possible levels of tumor targeting and cytotoxicity in ovarian cancer cells.

The analysis of in vivo apoptosis induction by different variants of a developed DDS supports previously reported findings related to the suppression of cellular antiapoptotic defense by BH3 peptide.[15,23,25,26,40–43] The proapoptotic activity of BH3 peptide increased after its conjugation to the PEG polymer and with the doubling of the number of copies of the peptide in the DDS. In addition to this expected result, we found that LHRH strengthened the ability of BH3 peptide to inhibit the synthesis of BCL2 protein and thus enhanced the induction of cell death by the anticancer drug. At the same time, an increase in the number of LHRH copies in a DDS containing CPT in the absence of the BH3 peptide led to the further overexpression of BCL2 protein. These phenomena may be explained by the increase in the bioavailability of the entire DDS and CPT, in particular by LHRH peptide initiating receptor-mediated endocytosis in LHRH receptor-expressing tumor cells. If BH3 peptide was not included in the LHRH receptor-targeted DDS, the higher bioavailability of CPT led to the higher level of compensative activation of cellular antiapoptotic defense when compared with that of the nontargeted CPT–PEG conjugate. The inclusion of BH3 peptide in a targeted DDS prevented such an activation.

The synergism among CPT, LHRH, and BH3 peptides included in one drug delivery system led to the higher antitumor activity of the entire multicomponent delivery system. Therefore, we were able to verify our hypothesis and show that simultaneous tumor targeting, apoptosis induction, and suppression of cellular antiapoptotic defense in tumor cells resulted in an increase in the antitumor activity of the entire complex to a level which cannot be achieved by individual components applied separately. In contrast to the existing drug delivery systems, the proposed DDS was effective in both sensitive and multidrug resistant tumors. However, in this study, the anticancer efficacy of the DDS was limited in P-glycoprotein-dependent multidrug resistant tumors. The suppression of such multidrug resistance should further enhance the antitumor efficacy of DDS in multidrug resistant tumors. The next generation of polymeric targeted proapoptotic DDS's is being currently developed in our laboratory. This will include, in addition to LHRH and BH3 peptides, suppressors of P-glycoprotein-dependent multidrug resistance (for instance, antisense oligonucleotides targeted to P-glycoprotein and/or multidrug resistance-associated protein mRNA previously used by us in liposomal delivery systems[27,29,44]). Evaluation of such complex multifunctional anticancer drug delivery system is a task for the future investigations.

Acknowledgment. The research was supported in part by NIH Grants CA100098, CA111766, and CA074175 from the National Cancer Institute. We thank Dr. Mikhail Kozlov (NanoTech Institute, University of Texas, Dallas, TX) for his advice on AFM imaging.

MP070053O

(40) Cosulich, S. C.; Worrall, V.; Hedge, P. J.; Green, S.; Clarke, P. R. Regulation of apoptosis by BH3 domains in a cell-free system. *Curr. Biol.* **1997**, *7*, 913–920.

(41) Lutz, R. J. Role of the BH3 (Bcl-2 homology 3) domain in the regulation of apoptosis and Bcl-2-related proteins. *Biochem. Soc. Trans.* **2000**, *28*, 51–56.

(42) Holinger, E. P.; Chittenden, T.; Lutz, R. J. Bak BH3 peptides antagonize Bcl-xL function and induce apoptosis through cytochrome c-independent activation of caspases. *J. Biol. Chem.* **1999**, *274*, 13298–13304.

(43) Schimmer, A. D.; Hedley, D. W.; Chow, S.; Pham, N. A.; Chakrabartty, A.; Bouchard, D.; Mak, T. W.; Trus, M. R.; Minden, M. D. The BH3 domain of BAD fused to the Antennapedia peptide induces apoptosis via its alpha helical structure and independent of Bcl-2. *Cell Death Differ.* **2001**, *8*, 725–733.

(44) Pakunlu, R. I.; Cook, T. J.; Minko, T. Simultaneous modulation of multidrug resistance and antiapoptotic cellular defense by MDR1 and BCL-2 targeted antisense oligonucleotides enhances the anticancer efficacy of doxorubicin. *Pharm. Res.* **2003**, *20*, 351–359.